Egyptian Journal of Chemistry
http://ejchem.journals.ekb.eg/

Chemical and Green Silver Nanoparticles: Synthesizing, Characterizing, and Antimicrobial Activity Against Microorganisms in Hatchery Plants

Nagwa H. Hamouda,[a*] Hanan F. Youssef,[b] W.D. Saleh,[a] Mohamed I. El Sabry,[c] and N.F. Nasr[a,]
[a]*Department of Microbiology, Faculty of Agriculture, Cairo University, 12613, Giza, Egypt.*
[b]*Ceramics, Refractories and Building Materials Department, National Research Centre (NRC), Dokki, 12622, Giza, Egypt.*
[c]*Department of Animal Production, Faculty of Agriculture, Cairo University, 12613, Giza, Egypt.*

Abstract

This work compares the characteristics and antimicrobial activity of chemically- and green-synthesized silver nanoparticles (Ag-NPs). The Ag-NPs were characterized using UV-visible spectroscopy, Fourier Transform Infrared Spectroscopy (FTIR) analyses, Transmission electron microscopy (TEM), and Zeta Potential (ZP). Results revealed that chemically synthesized Ag-NPs (C-Ag-NPs) were spherical with a particle size range of 4.86 to 13.6 nm, while the green-synthesized Ag-NPs (G-Ag-NPs) were of multi-shapes and size- range of 38.9 to 103 nm. Zone-inhibition test was done to compare the antimicrobial activity of both versions against common microbes of hatchery machines such as: G^+ bacteria (*Bacillus cereus*, *Bacillus subtilis*, *Staphylococcus aureus* and Methicillin-resistant *Staph. aureus* (MRSA), G^- bacteria (*Escherichia coli* O157; *Pseudomonas aeruginosa*, and *Salmonella typhimurium*), Mold (*Aspergillus niger*) and yeast (*Candida albicans*). Generally, both C-Ag-NPs and G-Ag-NPs had significant effects on the tested microbes. The antibacterial effect of G-Ag-NPs against *Ps. aeruginosa*, *B. cereus*, and MRSA was significantly stronger than that of C-Ag-NPs, while the antifungal effect of C-Ag-NPs against A*spergillus niger* was superior over that of G-Ag-NPs. For application, G-Ag-NPs and TH4 (a commercial disinfectant of poultry facilities) were separately sprayed onto the wall of egg incubators to compare their effect on total aerobic counts, total spore counts and total fungi. Results showed that both G-Ag-NPs and TH4 had strong effects on total aerobic counts, total spore-counts, and total fungi. G-Ag-NPs indicated higher efficacy than TH4. It could be concluded that G-Ag-NPs may be a promising antimicrobial candidate for sanitizing poultry facilities.

***Keywords*:** Nano-silver; antimicrobial activity; egg incubator; sanitization.

1. Introduction

Poultry diseases present a big challenge that hinders the improvement of the poultry industry, especially in developing countries [1–3]. A high load of pathogens including bacteria, molds, and yeasts could induce many diseases that negatively affect the health of the flocks, quality of baby chick, quality of meat, and poultry facility economics. For instance, Aspergillosis and Candidiasis are the most frequent fungal diseases in poultry that cause economic loss. Also, *Staphylococcus aureus* could increase morbidity and mortality in infected chicks [4–6].

Biosecurity strategy includes protocols preventing the introduction and/or spread of pathogens in poultry facilities. Sanitizers are a significant component of biosecurity protocols in which they are used for reducing surface microbial loads. Several commercial disinfectants have shown their efficacy however a number of them are not considered environmentally safe [7–9].

Over the last decades, silver nanoparticles (Ag-NPs) have gained importance due to their distinctive characteristics, such as chemical stability, catalytic and antimicrobial activities. These characteristics strongly impose Ag-NPs as an antimicrobial agent in several applications such as purifying water, pesticides and hatching egg sanitization [10,11]. Ag-

*Corresponding author e-mail: nagwa.hassan@agr.cu.edu.eg .; (Nagwa H. Hamouda).
Receive Date: 14 April 2022, Revise Date: 29 April 2022, Accept Date: 08 May 2022.
DOI: 10.21608/EJCHEM.2022.133474.5893

NPs with good biocidal properties may be an outstanding alternative to chemical disinfectants [8,12,13]. Synthesis and administration of chemically synthesized Ag-NPs (C-Ag-NPs) are may be criticized due to toxicity issues [14,15]. Consequently, finding efficient and environment-friendly methods for synthesizing metal nanoparticles became essential for safety reasons. The green synthesis methods have opened new horizons for finding eco-friendly nano products [16–18].

Therefore, this work was designed to synthesize silver nanoparticles chemically and biologically using trisodium citrate and mint (*Mentha piperita*) leaves-extract, respectively. Ag-NPs were characterized by spectroscopic analysis. The efficacy of the Ag-NPs against pathogens commonly present in poultry facilities was evaluated. Finally, a comparison between the effect of green-synthesized Ag-NPs (G-Ag-NPs) and TH4 on total aerobic bacterial counts, total spore counts and total fungi in poultry hatchery machines was carried out.

2. Experimental

2.1. Chemicals

Silver nitrate and Tri-sodium citrate dehydrate (Sigma-Aldrich-Schnelldorf, Germany) were used as delivered. The used commercial disinfectant (TH4) contained (g/L): 18.75 of dodecyl dimethyl ammonium chloride, 18.75 of dioctyl dimethyl ammonium chloride and 37.75 of octyl decyl dimethyl ammonium chloride, 50.0 of alkyl dimethyl benzyl ammonium chloride, 62.50 of glutaraldehyde, 20.0 of pine oil, and 20.0 of terpineol (Intercova Animal Health Products, France). Deionized water was used for dissolving the silver salt in all tests.

2.2. Synthesis of Ag-NPs

2.2.1. Chemical method

An aqueous solution of $AgNO_3$ was prepared by adding 0.1 g of silver nitrate to 100 mL deionized water and stirred, using magnetic rode and temperature- controlled magnetic stirrer. The $AgNO_3$ solution was heated up to boiling, and then 5 mL of 1% tri-sodium citrate dehydrate (TSC) solution were added drop-wise under continuous stirring. The reaction was allowed to take place until the solution color changed from yellow to greenish-yellow [19].

2.2.2. Green method

2.2.2.1. Preparation of mint-leaves extract

Leaves of mint, *Mentha piperita*, were gathered from the local market in Giza, Egypt, and were carefully washed using running tap water and rewashed with deionized water. The leaves were dried in a hot air oven at 50°C for 24 h and then were ground into powder using a mortar and pestle. The powder was stored for further use in airtight containers. For extraction, five grams of the leaves powder were suspended in 50 mL of sterilized deionized water and kept in a water bath at 100°C for 30 min. The extract was centrifuged at 5000 rpm for 15 min, and then filtered using Whatman filter paper No.1. The extract was filter-sterilized through a 0.22 µm pore size membrane filter and the sterilized extract was stored in a refrigerator at 4°C for further use [20].

2.2.2.2. Biosynthesis of Ag-NPs

Five mL of mint extract were mixed with 100 mL of silver nitrate solution. The mixture was heated at 90°C for 1 h, with constant stirring at 500 rpm, until the color changed from pale green to dark brown, and then stored under darkness at room temperature for 24 h to test the stability of Ag-NPs [20].

2.3. Characterization of Ag-NPs

2.3.1. UV-Vis spectral analysis

Spectral analysis for the development of Ag-NPs was conducted by ultraviolet-visible spectroscopy using UV- Vis Spectrophotometer (Cary100, Japan) in the range from 200 to 800 nm. The UV-visible spectroscopy was used to detect the Surface Plasmon Resonance (SPR) spectra of the synthesized nanomaterial; the reduction of $AgNO_3$ to nanoparticles is proven by the change in solution color from pale green to dark brown. This color change is mainly due to the SPR phenomenon. Metal nanoparticles have free electrons which give the SPR absorption band which is obtained by the combined oscillations of the electrons of the metal nanoparticles resonating with the light wave [21–26].

2.3.2. Fourier Transforms Infrared (FTIR) spectroscopy analysis

Functional groups of the synthesized Ag-NPs were detected using FTIR spectrometer (Infrared Spectrum Origin JASCO FT/IR-6100 typeA, Japan). Vacuum dried Ag-NPs were characterized in the range 400–4000 cm^{-1} at a resolution of 4 cm^{-1} using potassium bromide (KBr) pellet method. This helps

to characterize the potential molecules responsible for the reduction of Ag^+ ions and the stabilization of the reduced silver nanoparticles that prevent nanoparticles clustering and capping in the aqueous medium [27–30].

2.3.3. Transmission Electron Microscopy (TEM)

The average particle size and shape of Ag-NPs were determined using TEM (JEOL model JEM-2011) at the accelerating voltage of 80 kV. TEM samples of the reaction mixtures were prepared by placing 5 µl of the reaction mixtures over carbon-coated copper grids, allowing the samples to dry in a desiccator with silica to be examined [31].

2.3.4. Particle size and Zeta Potential Measurement

Zeta potential offers information about both the stability and surface charge of Ag-NPs in aqueous colloidal suspensions. The surface potential of the silver nanoparticles was determined using Particle Sizing Systems (ZPW388-V2.14, Inc. Santa Barbara, Calif., USA). Liquid samples of the Ag-NPs (5 mL) were diluted with double distilled water (50 mL) using NaCl as a suspending electrolyte solution (2 $x10^{-2}$ M NaCl). The pH was then adjusted to the required value at 7.0 ±0.2. The samples were shaken for 30 minutes, and then the Zeta Potential of the metallic particles was measured [32,33].

2.4. Antimicrobial activity of synthesized Ag-NPs

2.4.1. Determination of Ag-NPs antimicrobial activity

The chemical and green synthesized Ag-NPs were tested for their antimicrobial activity against the following target microorganisms: Gram positive bacteria; *Bacillus cereus* ATCC 33018, *Bacillus subtilis* ATCC 6633, and *Staphylococcus aureus* ATCC 25923; Methicillin-resistant *Staph. aureus* (MRSA) ATCC 43300. MRSA was kindly provided from Naval Medical Research Unit 3 (NAMRU-3). Also, their efficacy was tested against Gram negative bacteria; *Escherichia coli* ATCC 35218, *E. coli* O157 ATCC 700728; *Pseudomonas aeruginosa* ATCC 35032 and *Salmonella typhimurium* ATCC 14028, and the filamentous fungus *Aspergillus niger* NRRL 1957, along with the yeast *Candida albicans* ATCC 10231.

Pure microbial cultures were sub-cultured on Mueller Hinton (MH) agar [34] for bacteria and MH agar supplemented with 2% glucose for yeast and fungi. The antimicrobial activity of Ag-NPs was determined applying well-diffusion method on the same media using pour plate method. Wells of 10.0 mm in diameter were made using a sterile cork-borer, and then 20 µl of synthesized Ag-NPs were poured into each well. Plates were incubated at 30°C for 1 and 3 days for bacteria and fungi, respectively [35–37].

2.4.2. Efficacy of G-Ag-NPs versus TH4

The inside of the hatchery machine door was divided into 2 sections; each section was sprayed with either green Ag-NPs or TH4 at concentrations of 39 ppm and 2.0%, respectively. A sterile aluminum template (10×10 cm) was used to designate three sampling locations at each section. Sterilized cotton swabs were moistened by dipping in sterile 0.1% peptone water. Each location was wholly rubbed with moistened swab then the swabs were kept in a sample container containing 100 mL buffered peptone water (BPW). Each sample container was vortexed and stood for 20-30 min, and then serially diluted [38]. One mL of each dilution was aseptically inoculated into suitable media in triplicates, using pour plate method.

For determination of total aerobic and total spore counts, Standard plate count nutrient agar medium [34] was used at 30°C for 2 days. Rose Bengal chloramphenicol agar medium [34] was used for total fungi count at 30°C for 5 days. Counts of Enterobacteriaceae were detected on violet red bile glucose agar medium [34] for 2 days at 37°C. For total and fecal coliform, MPN method was applied using MacConkey broth medium [34] for 24h days at 37°C and 44.5°C, respectively.

For *Salmonella* detection, a pre-enrichment technique was performed in Buffered Peptone Water with incubating samples' bottles at 35°C for 24 h; ten mL of the pre-enriched (Buffered Peptone Water) BPW was transferred to inoculate 100 mL selenite cystine broth medium [34] for selective enrichment, and incubated at 43ºC for 24 h. A loop-full of each selenite cystine enrichment culture was streaked onto selective *Salmonella*/*Shigella* agar medium (SS agar) [34], and incubated at 37°C for 48 h [39–41].

2.5. Statistical analysis

Data were statistically analyzed using the linear model procedure (SAS, 2018). Differences were considered significant at $p < 0.05$. Differences among means were tested using Duncan's multiple range test [42]. The model applied was:

Yij = μ + Ti + Eij
Where:
Yij = Observations; μ = Overall mean; Ti = Effect of ith treatments; Eij = Experimental error

3. Results and discussion

3.1. Characterization of Ag-NPs

3.1.1. UV-Vis spectra analysis

Both chemically and biosynthetically prepared Ag-NPs were confirmed by UV–Vis spectral scanning in a range of 200–800 nm; the intensity of the surface plasmon resonance (SPR) band increased with time. Figure (1) is showing the UV results of both samples where the Ag-NPs peaks were found at different positions due to the sensitivity of the formed nanoparticles under varied reaction environment. The UV results of Ag-NPs synthesized using both chemical and green methods showed peaks at 418-420 and 390-400 nm, respectively. Results of C-Ag-NPs are in line with those of Van-Dong *et al.* and Agnihotri *et al.*, who assigned the peak at 420 nm wavelength for spherical Ag-NP with size 50 nm [43,44].

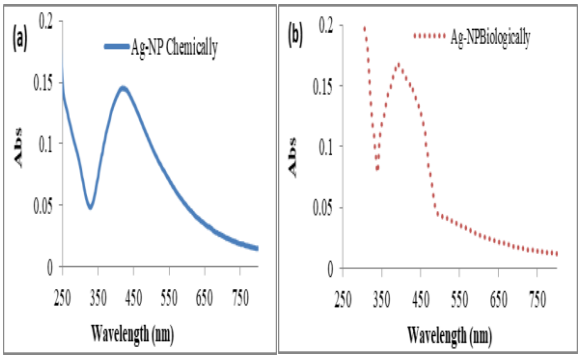

Fig. 1. UV–Visible absorption spectra of (a) C-Ag-NPs and (b) G-Ag-NPs.

Furthermore, the absorption spectra of G-Ag-NP in Fig. (1b) showed a large – sharp shoulder at about 400 nm, indicating large size and concentration of Ag-NPs compared to the chemical synthesis of Ag-NPs. These results are well consistent with Verma and Mehata, who investigated the biosynthesis of Ag-NPs observed at about 394 - 400 nm [45]. Moreover, Song *et al.* confirmed the correlation between the concentration of the Ag-NPs and the peak style where a weak peak indicates low concentration of the nanoparticles, meanwhile the increase in Ag-NPs concentration will be reflected in large plasmon peak intensity [46]. Accordingly, the main peaks of the tested samples showed large peaks and implied high silver nanoparticles concentration. The same authors demonstrated that the higher degree of nanoparticles dispersion will give the narrower plasmon peak. In accordance with the previous findings, the biosynthesis reaction for the Ag-NPs formation indicated larger particle sizes and higher concentration of Ag-NPs than that of the chemical derivation. The range 320-580 nm is a characteristic λ max for the bio-fabrication of Ag-NPs, as described by Hamouda *et al.*, whereby the frequency and bandwidth of the SPR depend not only on the size and shape of the metal nanoparticles, but also on the dielectric constant of the metal itself and the surrounding interfering medium [47]. It has been mentioned that phytochemicals present in plant extracts such as phenols, flavonoids, alkaloids, antioxidants, tannins, *etc.* might have a great influence on the biosynthesis of nanoparticles [48,49].

The UV-Vis spectrophotometry is the easy fast technique to confirm the synthesis, shape, size, concentration and dispersion of the Ag nanoparticles [46,50–52]. The change in the peak positioning for silver nanoparticles can be explained by the sensitivity of the produced Ag-NPs in different reaction environments. This effect normally reveals the difference in their distinguishing optical identities based on their SPR, which depends on the variation of nanoparticles' physical properties such as size and shape. The silver nanoparticles with changing size and shape have different numbers of free electrons at different energy levels. In addition, the interaction of those electrons results in the SPR absorption band, due to their combined oscillations in resonance with light waves. The reduction of $AgNO_3$ to nanoparticles is essentially indicated by the change in color of solutions from pale green to dark brown, for the green method, and from colorless to pale yellow in chemical preparation. Such change in color is commonly due to SPR [47,53].

3.1.2. FTIR spectroscopy analysis

The potential functional groups of the Chemo-/bio-synthesized granules of Ag-NPs, prepared from chemical and green reduction methods were characterized by FTIR and given in Fig. (2), respectively. Figure (2) presents the chemically synthesized product, C- Ag-NPs with the prominent peaks at 3453, 2922, 2864, 1647, 1490, 1451, 1395, 1127, 1054 and 562 cm^{-1}, assigning the presence of

the following chemical assemblies; OH stretching vibrations/carboxylic group, C-H stretching of alkanes, N-H bend of primary amines, stretching of C=O bonding, symmetrical stretching for N-O of nitro compounds (attributed to elemental function groups), –C–OCH_3 stretching modes of the alkyl halides and alkenes, respectively.

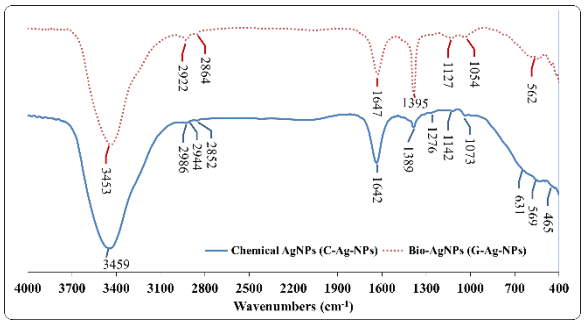

Fig. 2. FTIR of chemically and green synthesized Ag-NPs.

In comparison, the FTIR spectrum of G-Ag-NPs as shown in Fig. (2), where the characteristic IR peaks of the biologically produced silver nanoparticles were shifted to higher and lower wavenumbers 3459, 2986, 2944, 2852, 1642, 1389, 1276, 1142, 1156, 1073, 1057, 631, 569 and 465 cm^{-1} for the same structural groups mentioned above. These peaks signified the presence of vibrations of the following groups: O-H assigned for the phenol and/or carboxylic group in the plant extract; the stretching bond of C-H and N-H bending vibration from reducing and capping by plant extract at the bands 2986, 2944, 2852 cm^{-1}; stretching of C=O bonding at 1642 cm^{-1}; symmetrical stretching for N-O group of nitro compounds at 1389 cm^{-1}; C=N stretching vibration of aromatic amines at 1276 cm^{-1}; the elemental (sulfur or phosphorus) function groups presented at 1142, 1156, 1073, 1057 cm^{-1}, and the bending region of the aliphatic chain appeared at 631, 569 and 465 cm^{-1}, respectively.

Generally, the FTIR spectra usually reflect the significant variations of the peaks formed by different reducing agents. Accordingly, the peaks of G-Ag-NPs presented some characteristic bands to specify their biological nature, such as the assignment at 2986 cm^{-1} which refer to N-H bending vibration, also the strong peaks at 1389, 1276, 1156 and 631 cm^{-1} were distinguished from the reduction and capping the silver nanoparticles by the plant extract in the biosynthesis method.

Results of this work well-agree with the published data where the OH band found at 3459 cm^{-1} was reported at nearly the same position of 3441.01 cm^{-1} [53], 3401 cm^{-1} [54], and the absorbance bands around 3427-3436 cm^{-1} [47]. In addition, the stretching bond of C-H showed at the bands 2986, 2944, 2852 cm^{-1} are confirmed by Hamouda *et al*., where the peaks at 2924, 2854 and 1455 cm^{-1} were reported and may be attributed to aliphatic C-H stretching vibration of hydrocarbon chains and N-H bending vibration [47]. Moreover, the presence of the flavonoids and terpenoids in the plant extract were also investigated by Nithya Deva Krupa and Raghavan at intense assignments at 1645.28 cm^{-1} [53]. At the same time, Nithya Deva Krupa and Raghavan [53], Hamouda *et al*. [47], and Sadeghi and Gholamhoseinpoor [54], confirmed the bonding relationship between the free protein amides and the silver nanoparticles, to prevent the agglomeration of the prepared Ag-NPs by working as capping and stabilizing agent.

3.1.3. Transmission electron microscopy (TEM)

As depicted in Fig. (3 a, b), the TEM images clearly showed the size and shape of chemical and green synthesized nanoparticles of silver. C-Ag-NPs were found spherical in shape with an average size of 4.86 to 13.6 nm. G-Ag-NPs possessed different shapes as well as sizes including; spherical, triangular, irregular shapes with an average size of 38.9 to 103.0 nm.

The chemically prepared Ag-NPs are mostly homogeneous in size of less than 100 nm, and shape of nano-spheres, as can be seen in the C-Ag-NPs (Fig. 3a). The TEM testing investigations agree with

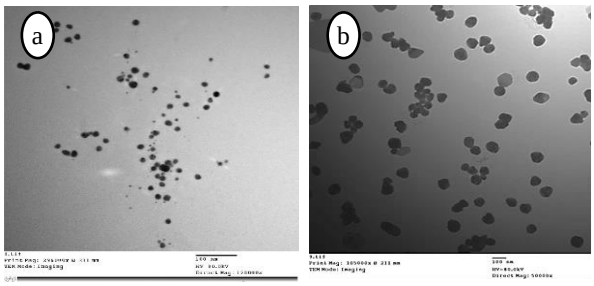

Fig. 3. TEM images of (a) C-Ag-NPs and (b) G-Ag-NPs.

those of Tonkovich groups and Guzman groups [19,55]. Meanwhile, the green methodology presented nanoparticles of G-Ag-NPs with different shapes of spherical, triangular, and irregular forms, and various particle sizes of >50 nm- micro and macro particles, as given in Fig. (3b). The difference

in size and shape of the G-Ag-NPs can result from the diversity of the mint extract components, which showed various reducing, chelating and binding characteristics. This postulation is supported by the findings of Gabriela *et al.* [20] and Klekotko *et al.* [56], who reported that the number of shapes given to the metallic nanoparticles is proportional to the amount of plant extract constituents in the reaction.

3.1.4. Particle size and Zeta-Potential measurements

3.1.4.1. Particle size

The particle-size distribution of chemical and green synthesized Ag-NPs is shown in Fig. 4 (a, b). The obtained data revealed the appearance of different peaks, such peaks with lower intensity matched to smaller nanoparticles and those of higher intensity matched to larger nanoparticles. Peaks of small nanoparticles were predominant in biosynthesized Ag-NPs compared to the chemically synthesized ones. In general, the mean diameters were 82.3 nm and 190.9 nm for the synthesized Ag-NPs by chemical and green methods, respectively.

The enlarged size of G-Ag-NPs may be attributed to the biomaterial compounds involved in the plant extract. These data confirm the above-mentioned results of UV and FTIR, where more homogenous and relatively uniformly-sized spherical-shaped granules with a narrow particle-size distribution of C-Ag-NPs, whereas G-Ag-NPs imply differently-shaped nanoparticles with a wider particle-size distribution. The mean diameter of C-Ag-NPs obtained in this study is about to be identical to that reported by Tomaszewska group [57], whereas, for G-Ag-NPs, Anandalakshmi group [58] and Gabriela group [20] reported particle sizes of up to 150 and 175 nm, respectively.

3.1.4.2. Zeta-Potential measurements

Zeta potential values obtained in the present study were -24.78 mV and -36.77 mV for chemical and green synthesized Ag-NPs, respectively (Fig. 5a and b). Zeta potential values provide good information on the surface charge and stability of the produced nanomaterials. When those values are negative, this ascertains the presence of repulsion forces among the particles and confirms their stable nature. The present C-Ag-NPs result is comparable to that reported by Yerraggopu team [59] who detected a value of -26 mV, whereas Farhadi and others reported –35 mV for G-Ag-NPs [60]. The difference in stability between C-Ag-NPs and G-Ag-NPs can be associated with phytochemical compounds of the mint extract. This was previously reported by many authors, who mentioned that those compounds can affect the stability of the metal nano particle molecules [20,48,49].

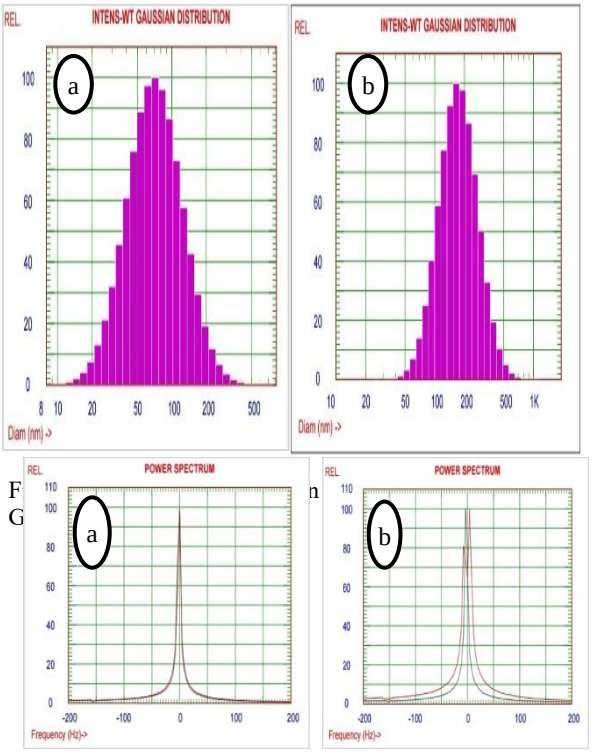

Fig. 5. Zeta potential values of (a) C-Ag-NPs and (b) G-Ag-NPs.

3.2. Antimicrobial activity of synthesized Ag-NPs

3.2.1. Determination of Ag-NPs antimicrobial activity

As shown in Table (1), both C-Ag-NPs and G-Ag-NPs, at the amount of 20 µl (bearing 50 ppm for C-Ag-NPs and 39 ppm for G-Ag-NPs), showed antimicrobial activities against all tested bacteria and fungi. No significant differences were found between the antimicrobial activity of C-Ag-NPs and that of G-Ag-NPs, however, the antibacterial effect of G- Ag-NPs against *Ps. aeruginosa, B. cereus* and *Staph. aureus* MRSA was significantly stronger than that of C-Ag-NPs. The antifungal effect of C-Ag-NPs against *Aspergillus niger* was superior over that of G-Ag-NPs. The highest inhibition zone was recorded with G-Ag-NPs against *C. albicans* (15.75 mm), while the lowest inhibition zone was recorded with

Table 1. Antimicrobial activities of C-Ag-NPs and G-Ag-NPs against studied G^- and G^+ bacteria and fungi.

Ag-NPs (20 µl)	Gram negative bacteria			
	E. coli	***E. coli O157***	***Ps. aeruginosa***	***S. typhimurium***
	Inhibition zone (mm)			
Chemical	**10.75[a]**	**11.57[a]**	**11.00[b]**	**11.50[a]**
Green	**12.50[a]**	**13.00[a]**	**12.25[a]**	**13.00[a]**
$LSD_{0.05}$	2.2056	1.8352	0.6117	1.8689
	Gram-positive bacteria			
	B. subtilis	***B. cereus***	***Staph. aureus***	***Staph. aureus* MRSA**
	Inhibition zone (mm)			
Chemical	**14.50[a]**	**11.50[b]**	**11.50[a]**	**11.25[b]**
Green	**12.00[a]**	**12.67[a]**	**12.00[a]**	**12.00[a]**
$LSD_{0.05}$	2.9124	1.1335	1.2235	0.6117
	Fungi			
	A. niger		***C. albicans***	
	Inhibition zone (mm)			
Chemical	**12.50[a]**		**15.50[a]**	
Green	**11.50[b]**		**15.75[a]**	
$LSD_{0.05}$	0.9989		1.9664	

[a,b]LSD followed by different letters, within row , differ significantly(p 0.05).

C-Ag-NPs against *E.coli* (10.75 mm).

Similar to these results, Logeswari *et al*. [61] reported that one hundred micro liters of G-Ag-NPs in well diffusion method revealed inhibition zones against pathogenic bacteria with the following diameters (mm): *Staphylococcus aureus* (30), *Pseudomonas aeruginosa* (25), *Escherichia coli* (30) and *Klebsiella pneumonia* (24). Hamed *et al.* [62] also deduced that G-Ag-NPs recorded significant antimicrobial effect against pathogenic bacteria, especially *Pseudomonas aeruginosa* with 18mm inhibition zone. Likewise, Savithramma *et al.* [63] found that G-Ag-NPs could significantly inhibit *Klebsiella*, *Pseudomonas*, *Aspergillus*, *Fusarium* and *Rhizopus*.

In this respect, many authors discussed physical and chemical properties of Ag-NPs including size, shape and surface charge as well as dose, and proved their antimicrobial activity [64–69]. Many suggested mechanisms described how the Ag-NPs cause their antagonistic effect; Some studies have reported that the charge of the Ag ion is crucial for its antimicrobial activity through the electric attraction between the cell membrane and the nanoparticles giving an opportunity to subsequent penetration and resulting in membrane permeability [70–73]. Dibrov *et al.* [72] proved the ability of Ag^+ to collapse the proton motive force resulting in a complete de-energization of the microbial cell membrane. This would result in a high degree of probability of cell death. In the same direction, Kim *et al.* [74] reported that free radicals, derived from the surface of Ag-NPs cause subsequent induction of membrane damage. Studying the effect of Ag-NPs on microbial DNA, Feng *et al.* [75] reported turning DNA into a condensed form in which the replication ability is lost and/or the interaction of silver ions with thiol groups in the proteins leading to inactivation of the cell enzymatic activities. In all cases, it should be noted that the mechanisms may differ depending on the bacterial species and the nano particle size.

3.2.2. Efficacy of G-Ag-NPs versus TH4

The control results showed that total aerobic bacterial count, total spores and total fungi, on the surface of the hatchery machine, were $2.2x10^6$, $2.8x10^5$ and $2.2x10^4$ CFU / cm^2, respectively. Post sanitation results (30 min after spraying) showed that TH4 reduced the total bacterial counts, spore counts, and total fungi by 87.72%, 92.50%, and 71.36%, in that order. On the other hand, G-Ag-NPs succeeded to reduce those numbers by 99.93%, 99.98%, and 99.93% (Fig. 6).

No *Salmonella typhimurium*, Entrobacteriaceae, total coliform or fecal coliform were detected in the control. This generally indicates good hygienic conditions, as mentioned by Musgrove *et al.* [76].

Monitoring the stability of the used disinfectants after 3 days of sanitation, by determining the same parameters (total aerobic bacteria, total spores, and total fungi counts), revealed that all readings of G-Ag-NPs remained at the same levels, whereas the efficacy of TH4 against total aerobic bacteria dropped

by about 10% and by about 4.3%, for total spore counts. The activity of TH4 against total fungi, after 3 days, was found to increase from 71.36% to 98.86%. This may indicate slow action of TH4 against fungi, but, even though, G-Ag-NPs were still superior (Fig. 6). The different bacterial and fungal responses have previously been reported by others [77,78]. The difference between bacterial and fungal responses can be related to the general observation that eukaryotic and prokaryotic microorganisms display different degrees of sensitivity [79–81].

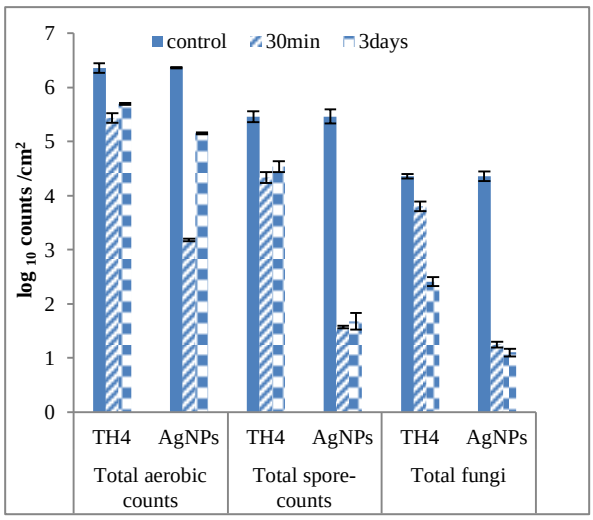

Fig. 6. Effect of G-Ag-NPs and TH4 on total bacteria, total spores, and total fungi counts on the hatchery machine surface.

In poultry hatcheries, restrict hygiene practices are followed to minimize pathogenic microorganisms that infect the embryos in fertile eggs and newly hatched chicks. Therefore, different disinfectants are utilized for lowering the microbial load on the eggshell, egg incubator and hatchery surfaces. Thus, many trials have been conducted to find out new disinfectants and/or improve generations of them to control the resistant strains of microorganisms on eggshell and hatchery surfaces [82,83].

4. Conclusion

In conclusion, both chemically and green synthesized Ag-NPs have significant antimicrobial effects on the tested G^+ and G^- bacteria and fungi. The antimicrobial activity of green Ag-NPs is higher than that of TH4. Regarding the potentiality of present results, green Ag-NPs, could be suggested as a promising sanitizer for the machines in poultry hatchery plants. However, more toxicological and environmental studies should be done to investigate the safety of green Ag-NPs.

5. Conflicts of interest

The authors have no conflict of interest.

6. References

[1] El-Sabry, M. I. M., Atta, A. M. M., Tzschentke, B., Gharib, H. B. A., and Stino, F. K. R. (2012). Potential Use of Interleukin-2-Rich Supernatant Adjuvant in Fayoumi Hens. Arch. Fur Geflugelkd., **76**: 162–167 .

[2] Mehaisen, G. M. K., Eshak, M. G., El Sabry, M. I., and Abass, A. O. (2016). Expression of Inflammatory and Cell Death Program Genes and Comet DNA Damage Assay Induced by Escherichia Coli in Layer Hens. PLoS One, **11**(6): e0158314 .

[3] Parrott, P., and Walley, K. (2017). Chapter 13 - Consumer Attitudes to Poultry Meat: A Comparative Study of the UK and China. , *Woodhead Publishing Series in Food Science, Technology and Nutrition*, M. Petracci, and C.B.T.-P.Q.E. Berri, eds., Woodhead Publishing, 313–334 .

[4] Stringfellow, K., Anderson, P., Caldwell, D., Lee, J., Byrd, J., McReynolds, J., Carey, J., Nisbet, D., and Farnell, M. (2009). Evaluation of Disinfectants Commonly Used by the Commercial Poultry Industry under Simulated Field Conditions. Poult. Sci., **88**(6): 1151–1155 .

[5] Osman, K. M., Kappell, A. D., Elhadidy, M., ElMougy, F., El-Ghany, W. A. A., Orabi, A., Mubarak, A. S., Dawoud, T. M., Hemeg, H. A., and Moussa, I. M. I. (2018). Poultry Hatcheries as Potential Reservoirs for Antimicrobial-Resistant *Escherichia coli*: A Risk to Public Health and Food Safety. Sci. Rep., **8**(1): 1–14 .

[6] Szafraniec, G. M., Szeleszczuk, P., and Dolka, B. (2020). A Review of Current Knowledge on *Staphylococcus agnetis* in Poultry. Animals, **10**(8): 1421 .

[7] Ramesh, N., Viswanathan, M. B., Saraswathy, A., Balakrishna, K., Brindha, P., and Lakshmanaperumalsamy, P. (2002). Phytochemical and Antimicrobial Studies of *Begonia malabarica*. J. Ethnopharmacol., **79**(1): 129–132 .

[8] Deshmukh, P., Li, J., Nalamati, S., Sharma, M., and Iyer, S. (2019). Molecular Beam Epitaxial Growth of GaAsSb/GaAsSbN/GaAlAs Core-Multishell Nanowires for near-Infrared Applications. Nanotechnology, **30**(27): 275203 .

[9] Saha, O., Rakhi, N. N., Istiaq, A., Islam, I., Sultana, M., Hossain, M. A., and Rahaman, M.

(2020). Evaluation of Commercial Disinfectants against *Staphylococcus lentus* and *Micrococcus* Spp. of Poultry Origin. Vet. Med. Int., **2020**: 1–10

[10] Babu, M. M. G., and Gunasekaran, P. (2013). Extracellular Synthesis of Crystalline Silver Nanoparticles and Its Characterization. Mater. Lett., **90**: 162–164 .

[11] Ibrahim, F. A., Elkloub, K., Moustafa, M. E., El Sabry, M. I., Jihan, M. B., and Hassan, A. S. I. (2018). Effect of Egg Disinfection by Silver Nanoparticles on Eggshell Microbial Load, Hatchability and Post-Hatch Performance of Quail Chicks. Int. J. Poult. Sci., **17**: 234–242 .

[12] Konopka, M., Kowalski, Z., and Wzorek, Z. (2009). Disinfection of Meat Industry Equipment and Production Rooms with the Use of Liquids Containing Silver Nano-Particles. Arch. Environ. Prot., **35**(1): 107–115 .

[13] Metak, A. M., and Ajaal, T. T. (2013). Investigation on Polymer Based Nano-Silver as Food Packaging Materials. Int. J. Chem. Mol. Eng., **7**(12): 1103–1109 .

[14] Roy, N., Gaur, A., Jain, A., Bhattacharya, S., and Rani, V. (2013). Green Synthesis of Silver Nanoparticles: An Approach to Overcome Toxicity. Environ. Toxicol. Pharmacol., **36**(3): 807–812 .

[15] Khoshnamvand, M., Hao, Z., Fadare, O. O., Hanachi, P., Chen, Y., and Liu, J. (2020). Toxicity of Biosynthesized Silver Nanoparticles to Aquatic Organisms of Different Trophic Levels. Chemosphere, **258**: 127346 .

[16] Akhtar, M. S., Panwar, J., and Yun, Y. S. (2013). Biogenic Synthesis of Metallic Nanoparticles by Plant Extracts. ACS Sustain. Chem. Eng., **1**(6): 591–602 .

[17] El-Sabry, M. I., McMillin, K. W., and Sabliov, C. M. (2018). Nanotechnology Considerations for Poultry and Livestock Production Systems–a Review. Ann. Anim. Sci., **18**(2): 319–334 .

[18] Castillo-Henríquez, L., Alfaro-Aguilar, K., Ugalde-Álvarez, J., Vega-Fernández, L., Montes de Oca-Vásquez, G., and Vega-Baudrit, J. R. (2020). Green Synthesis of Gold and Silver Nanoparticles from Plant Extracts and Their Possible Applications as Antimicrobial Agents in the Agricultural Area. Nanomaterials, **10**(9): 1763

[19] Turkevich, J., Stevenson, P. C., and Hillier, J. (1951). A Study of the Nucleation and Growth Processes in the Synthesis of Colloidal Gold. Discuss. Faraday Soc., **11**: 55–75 .

[20] Gabriela, Á.-M., Gabriela, M. de O.-V., Luis, A.-M., Reinaldo, P.-R., Michael, H.-M., Rodolfo, G.-P., and Roberto, V.-B. J. (2017). Biosynthesis of Silver Nanoparticles Using Mint Leaf Extract (*Mentha piperita*) and Their Antibacterial Activity. Adv. Sci. Eng. Med., **9**(11): 914–923 .

[21] Link, S., and El-Sayed, M. A. (2003). Optical Properties and Ultrafast Dynamics of Metallic Nanocrystals. Annu. Rev. Phys. Chem., **54**(1): 331–366 .

[22] Jaidev, L. R., and Narasimha, G. (2010). Fungal Mediated Biosynthesis of Silver Nanoparticles, Characterization and Antimicrobial Activity. Colloids Surfaces B Biointerfaces, **81**(2): 430–433 .

[23] Baset, S., Akbari, H., Zeynali, H., and Shafie, M. (2011). Size Measurement of Metal and Semiconductor Nanoparticles *via* Uv-Vis Absorption Spectra. Dig. J. Nanomater. Biostructures, **6**(2): 709–716 .

[24] Devaraj, P., Kumari, P., Aarti, C., and Renganathan, A. (2013). Synthesis and Characterization of Silver Nanoparticles Using Cannonball Leaves and Their Cytotoxic Activity against MCF-7 Cell Line. J. Nanotechnol., **2013**: 1–5 .

[25] Kosuda, K., Bingham, J., Wustholz, K., and Van Duyne, R. (2010). Nanostructures and Surface-Enhanced Raman Spectroscopy. Handb. Nanoscale Opt. Electron., **3**: 309–346 .

[26] Pryshchepa, O., Pomastowski, P., and Buszewski, B. (2020). Silver Nanoparticles: Synthesis, Investigation Techniques, and Properties. Adv. Colloid Interface Sci., **284**: 102246 .

[27] Basavaraja, S., Balaji, S. D., Lagashetty, A., Rajasab, A. H., and Venkataraman, A. (2008). Extracellular Biosynthesis of Silver Nanoparticles Using the Fungus *Fusarium semitectum*. Mater. Res. Bull., **43**(5): 1164–1170 .

[28] Velmurugan, P., Park, J.-H., Lee, S.-M., Jang, J.-S., Lee, K.-J., Han, S.-S., Lee, S.-H., Cho, M., and Oh, B.-T. (2015). Synthesis and Characterization of Nanosilver with Antibacterial Properties Using Pinus Densiflora Young Cone Extract. J. Photochem. Photobiol. B Biol., **147**: 63–68 .

[29] Faghihzadeh, F., Anaya, N. M., Schifman, L. A., and Oyanedel-Craver, V. (2016). Fourier Transform Infrared Spectroscopy to Assess Molecular-Level Changes in Microorganisms Exposed to Nanoparticles. Nanotechnol. Environ. Eng., **1**(1): 1–16 .

[30] Karthik, C., Suresh, S., Mirulalini, S., and Kavitha, S. (2020). A FTIR Approach of Green Synthesized Silver Nanoparticles by *Ocimum sanctum* and *Ocimum gratissimum* on Mung Bean Seeds. Inorg. Nano-Metal Chem., **50**(8): 606–612

[31] Eskandari, M. J., Gostariani, R., and Asadabad, M. A. (2020). Transmission Electron Microscopy of Nanomaterials. , Electron Crystallography, IntechOpen, 9–26 .

[32] Shnoudeh, A. J., Hamad, I., Abdo, R. W., Qadumii, L., Jaber, A. Y., Surchi, H. S., and Alkelany, S. Z. (2019). Synthesis, Characterization, and Applications of Metal Nanoparticles. Biomaterials and Bionanotechnology, Elsevier, 527–612 .

[33] Mateos, H., Picca, R. A., Mallardi, A., Dell'Aglio, M., De Giacomo, A., Cioffi, N., and Palazzo, G. (2020). Effect of the Surface Chemical Composition and of Added Metal Cation Concentration on the Stability of Metal Nanoparticles Synthesized by Pulsed Laser Ablation in Water. Appl. Sci., **10**(12): 4169 .

[34] Atlas, R. M. (2006). The Handbook of Microbiological Media for the Examination of Food., CRC press.

[35] Alastruey-Izquierdo, A., Melhem, M. S. C., Bonfietti, L. X., and Rodriguez-Tudela, J. L. (2015). Susceptibility Test for Fungi: Clinical and Laboratorial Correlations in Medical Mycology. Rev. Inst. Med. Trop. Sao Paulo, **57**: 57–64 .

[36] Feroze, N., Arshad, B., Younas, M., Afridi, M. I., Saqib, S., and Ayaz, A. (2020). Fungal Mediated Synthesis of Silver Nanoparticles and Evaluation of Antibacterial Activity. Microsc. Res. Tech., **83**(1): 72–80 .

[37] Huq, M. (2020). Green Synthesis of Silver Nanoparticles Using *Pseudoduganella eburnea* MAHUQ-39 and Their Antimicrobial Mechanisms Investigation against Drug Resistant Human Pathogens. Int. J. Mol. Sci., **21**(4): 1510 .

[38] Collins, C. H. (1967). Microbiological Methods. Microbiol. methods., (2nd Edition): .

[39] Kim, J. Y., Bahnson, P., Kakoma, I., and Isaacson, R. (1999). The Effect of Buffered Peptone Water Pre-Enrichment on Detected Prevalence of *Salmonella* in Swine Feces. 69–71 .

[40] Garibo, D., Borbón-Nuñez, H. A., de León, J. N. D., García Mendoza, E., Estrada, I., Toledano-Magaña, Y., Tiznado, H., Ovalle-Marroquin, M., Soto-Ramos, A. G., and Blanco, A. (2020). Green Synthesis of Silver Nanoparticles Using *Lysiloma acapulcensis* Exhibit High-Antimicrobial Activity. Sci. Rep., **10**(1): 1–11 .

[41] Ríos-Castillo, A. G., Ripolles-Avila, C., and Rodríguez-Jerez, J. J. (2020). Detection of S*almonella typhimurium* and *Listeria monocytogenes* Biofilm Cells Exposed to Different Drying and Pre-Enrichment Times Using Conventional and Rapid Methods. Int. J. Food Microbiol., **324**: 108611 .

[42] Duncan, D. B. (1955). Multiple Range and Multiple F Tests. Biometrics, **11**(1): 1–42 .

[43] Agnihotri, S., Mukherji, S., and Mukherji, S. (2014). Size-Controlled Silver Nanoparticles Synthesized over the Range 5–100 Nm Using the Same Protocol and Their Antibacterial Efficacy. Rsc Adv., **4**(8): 3974–3983 .

[44] Van-Dong, P., Ha, C. H., Binh, L. T., and Kasbohm, J. (2012). Chemical Synthesis and Antibacterial Activity of Novel-Shaped Silver Nanoparticles. Int. Nano Lett., **2**(1): 2–9 .

[45] Verma, A., and Mehata, M. S. (2016). Controllable Synthesis of Silver Nanoparticles Using Neem Leaves and Their Antimicrobial Activity. J. Radiat. Res. Appl. Sci., **9**(1): 109–115

[46] Song, K. C., Lee, S. M., Park, T. S., and Lee, B. S. (2009). Preparation of Colloidal Silver Nanoparticles by Chemical Reduction Method. Korean J. Chem. Eng. 2009 261, **26**(1): 153–155 .

[47] Hamouda, R. A., Hussein, M. H., Abo-elmagd, R. A., and Bawazir, S. S. (2019). Synthesis and Biological Characterization of Silver Nanoparticles Derived from the Cyanobacterium *Oscillatoria limnetica*. Sci. Rep., **9**(1): 1–17 .

[48] Chaudhuri, S. K., Chandela, S., and Malodia, L. (2016). Plant Mediated Green Synthesis of Silver Nanoparticles Using Tecomella Undulata Leaf Extract and Their Characterization. Nano Biomed. Eng., **8**(1): 1–8 .

[49] Ovais, M., Khalil, A. T., Islam, N. U., Ahmad, I., Ayaz, M., Saravanan, M., Shinwari, Z. K., and Mukherjee, S. (2018). Role of Plant Phytochemicals and Microbial Enzymes in Biosynthesis of Metallic Nanoparticles. Appl. Microbiol. Biotechnol., **102**(16): 6799–6814 .

[50] Lee, K.-S., and El-Sayed, M. A. (2005). Dependence of the Enhanced Optical Scattering Efficiency Relative to That of Absorption for Gold Metal Nanorods on Aspect Ratio, Size, End-Cap Shape, and Medium Refractive Index. J. Phys. Chem. B, **109**(43): 20331–20338 .

[51] Skiba, M., Pivovarov, A., Makarova, A., and Vorobyova, V. (2018). Plasma-Chemical Synthesis of Silver Nanoparticles in the Presence of Citrate. Chem. J. Mold., **13**(1): 7–14 .

[52] Trang, N. L. N., Hoang, V.-T., Dinh, N. X., Tam, L. T., Le, V. P., Linh, D. T., Cuong, D. M., Khi, N. T., Anh, N. H., Nhung, P. T., and Le, A.-T. (2021). Novel Eco-Friendly Synthesis of Biosilver Nanoparticles as a Colorimetric Probe for Highly Selective Detection of Fe (III) Ions in Aqueous Solution. J. Nanomater., **2021**: 5527519.

[53] Nithya-Deva-Krupa, A., and Raghavan, V. (2014). Biosynthesis of Silver Nanoparticles Using *Aegle marmelos* (Bael) Fruit Extract and Its Application to Prevent Adhesion of Bacteria: A Strategy to Control Microfouling. Bioinorg. Chem. Appl., **2014**: 949538 .

[54] Sadeghi, B., and Gholamhoseinpoor, F. (2015). A Study on the Stability and Green Synthesis of Silver Nanoparticles Using *Ziziphora tenuior* (Zt) Extract at Room Temperature. Spectrochim. Acta Part A Mol. Biomol. Spectrosc., **134**: 310–315 .

[55] Guzmán, M. G., Dille, J., and Godet, S. (2009). Synthesis of Silver Nanoparticles by Chemical Reduction Method and Their Antibacterial Activity. Int J Chem Biomol Eng, **2**(3): 104–111 .

[56] Klekotko, M., Matczyszyn, K., Siednienko, J., Olesiak-Banska, J., Pawlik, K., and Samoc, M. (2015). Bio-Mediated Synthesis, Characterization and Cytotoxicity of Gold Nanoparticles. Phys. Chem. Chem. Phys., **17**(43): 29014–29019 .

[57] Tomaszewska, E., Soliwoda, K., Kadziola, K., Tkacz-Szczesna, B., Celichowski, G., Cichomski, M., Szmaja, W., and Grobelny, J. (2013). Detection Limits of DLS and UV-Vis Spectroscopy in Characterization of Polydisperse Nanoparticles Colloids. J. Nanomater., **2013**: 1–10 .

[58] Anandalakshmi, K., Venugobal, J., and Ramasamy, V. (2016). Characterization of Silver Nanoparticles by Green Synthesis Method Using *Pedalium murex* Leaf Extract and Their Antibacterial Activity. Appl. Nanosci., **6**(3): 399–408 .

[59] Yerragopu, P. S., Hiregoudar, S., Nidoni, U., Ramappa, K. T., Sreenivas, A. G., and Doddagoudar, S. R. (2020). Chemical Synthesis of Silver Nanoparticles Using Tri-Sodium Citrate, Stability Study and Their Characterization. Int. Res. J. Pure Appl. Chem., **21**(3): 37–50 .

[60] Farhadi, S., Ajerloo, B., and Mohammadi, A. (2017). Green Biosynthesis of Spherical Silver Nanoparticles by Using Date Palm (*Phoenix dactylifera*) Fruit Extract and Study of Their Antibacterial and Catalytic Activities. Acta Chim. Slov., **64**(1): 129–143 .

[61] Logeswari, P., Silambarasan, S., and Abraham, J. (2015). Synthesis of Silver Nanoparticles Using Plants Extract and Analysis of Their Antimicrobial Property. J. Saudi Chem. Soc., **19**(3): 311–317 .

[62] Hamed, A. A., Kabary, H., Khedr, M., and Emam, A. N. (2020). Antibiofilm, Antimicrobial and Cytotoxic Activity of Extracellular Green-Synthesized Silver Nanoparticles by Two Marine-Derived Actinomycete. RSC Adv., **10**(17): 10361–10367 .

[63] Savithramma, N., Rao, M. L., Rukmini, K., and Devi, P. S. (2011). Antimicrobial Activity of Silver Nanoparticles Synthesized by Using Medicinal Plants. Int. J. ChemTech Res., **3**(3): 1394–1402 .

[64] Shrivastava, S., Bera, T., Roy, A., Singh, G., Ramachandrarao, P., and Dash, D. (2007). Characterization of Enhanced Antibacterial Effects of Novel Silver Nanoparticles. Nanotechnology, **18**(22): 225103 .

[65] Gopinath, V., MubarakAli, D., Priyadarshini, S., Priyadharsshini, N. M., Thajuddin, N., and Velusamy, P. (2012). Biosynthesis of Silver Nanoparticles from *Tribulus terrestris* and Its Antimicrobial Activity: A Novel Biological Approach. Colloids surfaces B biointerfaces, **96**: 69–74 .

[66] Logeswari, P., Silambarasan, S., and Abraham, J. (2013). Ecofriendly Synthesis of Silver Nanoparticles from Commercially Available Plant Powders and Their Antibacterial Properties. Sci. Iran., **20**(3): 1049–1054 .

[67] Peters, R. J. B., Bouwmeester, H., Gottardo, S., Amenta, V., Arena, M., Brandhoff, P., Marvin, H. J. P., Mech, A., Moniz, F. B., and Pesudo, L. Q. (2016). Nanomaterials for Products and Application in Agriculture, Feed and Food. Trends Food Sci. Technol., **54**: 155–164 .

[68] Cheon, J. Y., Kim, S. J., Rhee, Y. H., Kwon, O. H., and Park, W. H. (2019). Shape-Dependent Antimicrobial Activities of Silver Nanoparticles. Int. J. Nanomedicine, **14**: 2773 .

[69] Choi, J. S., Lee, J. W., Shin, U. C., Lee, M. W., Kim, D. J., and Kim, S. W. (2019). Inhibitory Activity of Silver Nanoparticles Synthesized Using *Lycopersicon esculentum* against Biofilm Formation in Candida Species. Nanomaterials, **9**(11): 1512 .

[70] Dragieva, I., Stoeva, S., Stoimenov, P., Pavlikianov, E., and Klabunde, K. (1999). Complex Formation in Solutions for Chemical Synthesis of Nanoscaled Particles Prepared by Borohydride Reduction Process. Nanostructured Mater., **12**(1–4): 267–270 .

[71] Hamouda, T., Myc, A., Donovan, B., Shih, A. Y., Reuter, J. D., and Baker, J. R. (2001). A Novel Surfactant Nanoemulsion with a Unique Non-Irritant Topical Antimicrobial Activity against Bacteria, Enveloped Viruses and Fungi. Microbiol. Res., **156**(1): 1–7 .

[72] Dibrov, P., Dzioba, J., Gosink, K. K., and Häse, C. C. (2002). Chemiosmotic Mechanism of Antimicrobial Activity of Ag+ in *Vibrio cholerae*. Antimicrob. Agents Chemother., **46**(8): 2668–

2670 .

[73] Morones, J. R., Elechiguerra, J. L., Camacho, A., Holt, K., Kouri, J. B., Ramirez, J. [74] Kim, J. S., Kuk, E., Yu, K. N., Kim, J.-H., Park, S. J., Lee, H. J., Kim, S. H., Park, Y. K., Park, Y. H., and Hwang, C.-Y. (2007). Antimicrobial Effects of Silver Nanoparticles. Nanomedicine Nanotechnology, Biol. Med., **3**(1): 95–101 .

[75] Feng, J., Shi, J., Sirimanne, S. R., Mounier-lee, C. E., and May, S. W. (2000). Kinetic and Stereochemical Studies on Novel Inactivators of C-Terminal. Amidation. **530**: 521–530 .

[76] Musgrove, M. T., Stephens, C. B., Bourassa, D. V, Cox, N. A., Mauldin, J. M., Berrang, M. E., and Buhr, R. J. (2014). *Enterobacteriaceae* and *Salmonella* Recovered from Nonsanitized and Sanitized Broiler Hatching Eggs. J. Appl. Poult. Res., **23**(3): 516–522 .

[77] Gryndler, M., Hršelová, H., Soukupová, L., and Borovička, J. (2012). Silver Release from Decomposed Hyperaccumulating *Amanita solitaria* Fruit-Body Biomass Strongly Affects Soil Microbial Community. Biometals, **25**(5): 987–993 .

[78] Kumar, N., Palmer, G. R., Shah, V., and Walker, V. K. (2014). The Effect of Silver Nanoparticles on Seasonal Change in Arctic Tundra Bacterial and Fungal Assemblages. PLoS One, **9**(6): e99953 .

T., and Yacaman, M. J. (2005). The Bactericidal Effect of Silver Nanoparticles. Nanotechnology, **16**(10): 2346 .

[79] Brake, J., and Sheldon, B. W. (1990). Effect of a Quaternary Ammonium Sanitizer for Hatching Eggs on Their Contamination, Permeability, Water Loss, and Hatchability. Poult. Sci., **69**(4): 517–525 .

[80] Sotohy, S. A., and Mohamed, A. A. (1999). Fungicidal Effect of the Common Disinfectants on the Most Widely Spread Dermatophytes with References to Their Differential Resistance “in-Vitro” Study. Assiut Vet. Med. J., **41**(81): 113–126 .

[81] Sillen, W. M. A., Thijs, S., Abbamondi, G. R., Janssen, J., Weyens, N., White, J. C., and Vangronsveld, J. (2015). Effects of Silver Nanoparticles on Soil Microorganisms and Maize Biomass Are Linked in the Rhizosphere. Soil Biol. Biochem., **91**: 14–22 .

[82] Oliveira, G. da S., Nascimento, S. T., Dos Santos, V. M., and Silva, M. G. (2020). Clove Essential Oil in the Sanitation of Fertile Eggs. Poult. Sci., **99**(11): 5509–5516 .

[83] Shang, K., Wei, B., Cha, S.-Y., Zhang, J.-F., Park, J.-Y., Lee, Y.-J., Jang, H.-K., and Kang, M. (2021). The Occurrence of Antimicrobial-Resistant *Salmonella enterica* in Hatcheries and Dissemination in an Integrated Broiler Chicken Operation in Korea. Animals, **11**(1): 154 .